USGS
science for a changing world

Summary of Oceanographic and Water-Quality Measurements Offshore of Matanzas Inlet, Florida, 2018

Open-File Report 2021–1014

U.S. Department of the Interior
U.S. Geological Survey

Cover. Instrumented sea-floor platform ready for deployment. Photograph by Ellyn Montgomery, U.S. Geological Survey.

Summary of Oceanographic and Water-Quality Measurements Offshore of Matanzas Inlet, Florida, 2018

By Marinna A. Martini, Ellyn T. Montgomery, Steven E. Suttles, and John C. Warner

Open-File Report 2021–1014

U.S. Department of the Interior
U.S. Geological Survey

U.S. Geological Survey, Reston, Virginia: 2021

Suggested citation:
Martini, M.A., Montgomery, E.T., Suttles, S.E., and Warner, J.C., 2021, Summary of oceanographic and water-quality measurements offshore of Matanzas Inlet, Florida, 2018: U.S. Geological Survey Open-File Report 2021–1014, 21 p., https://doi.org/10.3133/ofr20211014.

Associated data for this publication:
Suttles, S.E., Warner, J.C., Montgomery, E.T., and Martini, M.A., 2019, Oceanographic and water quality measurements in the nearshore zone at Matanzas Inlet, Florida, January–April, 2018: U.S. Geological Survey data release, https://doi.org/10.5066/P9GKB537.

Suttles, S.E., De Meo, O.A., Martini, M.A, and Warner, J.C., 2021, Grain-size analysis data from sediment samples in support of oceanographic and water-quality measurements in the nearshore zone of Matanzas Inlet, Florida, 2018—U.S. Geological Survey Field Activity: U.S. Geological Survey data release, https://doi.org/10.5066/P9FKARIZ.

ISSN 2331-1258 (online)

Acknowledgments

This research was conducted as part of the U.S. Geological Survey Cross-Shore and Inlets Processes study of the processes controlling coastal sediment transport. The Skidaway Institute of Oceanography, University of Georgia, provided vessel and field support that were an essential part of this work. The officers and crew of the research vessel *Savannah* ably supported the scientific mission with expert ship-handling in challenging conditions. Marine Superintendent John Bichy provided expert assistance with logistics and shipping. The authors would also like to acknowledge the field, logistical, and analytic support provided by Jonathan Borden, Eric Marsjanik, and Brian Buczkowski of the U.S. Geological Survey.

Contents

Figures

Tables

Conversion Factors

International System of Units to U.S. Customary Units

Multiply	By	To obtain
	Length	
centimeter (cm)	0.39370	inch (in)
millimeter (mm)	0.03937	inch (in)
meter (m)	3.28100	foot (ft)
kilometer (km)	0.62140	mile, U.S. statute (mi)
kilometer (km)	0.54000	mile, nautical (nmi)
	Pressure	
decibar (dbar)	1.45000	pound per square inch (lb/in^2)
millibar (mbar)	0.02953	inch of mercury at 32°F (inHg)
hectopascal (hPa)	0.0145	pound per square inch (lb/in^2)

Temperature in degrees Celsius (°C) may be converted to degrees Fahrenheit (°F) as

$$°F = (1.8 \times °C) + 32.$$

Datum

Horizontal coordinate information is referenced to the World Geodetic System of 1984 (WGS 84).

Supplemental Information

Pressure measured underwater is given in decibars (dbar).

Current speed is given in centimeters per second (cm/s).

Current direction is given in degrees, as direction to which the water is flowing, measured clockwise from North (degrees).

Wind speed is given in meters per second (m/s).

Wave direction is given in degrees, as coming from which waves are propagating, measured clockwise from North (degrees).

Turbidity is given in nephelometric turbidity units (NTU).

Salinity is given as practical salinity units (PSU).

Irradiance is given in watts per square meter (W/m^2).

Conductivity is given in siemens per meter (S/m).

Sound is given in decibels (dB).

Abbreviations

ABSS	acoustic backscatter sensor
ADCP	acoustic Doppler current profiler
ADV	acoustic Doppler velocimeter
HR	high resolution
Hz	hertz
MHz	megahertz
mab	meters above bottom
netCDF	Network Common Data Form

Summary of Oceanographic and Water-Quality Measurements Offshore of Matanzas Inlet, Florida, 2018

By Marinna A. Martini, Ellyn T. Montgomery, Steven E. Suttles, and John C. Warner

Abstract

U.S. Geological Survey (USGS) scientists and technical staff deployed instrumented underwater platforms and buoys to collect oceanographic and atmospheric data at two sites near Matanzas Inlet, Florida, on January 24, 2018, and recovered them on April 13, 2018. Matanzas Inlet is a natural, unmaintained inlet on the Florida Atlantic coast that is well suited to study inlet and cross-shore processes. The two study sites were located offshore of the surf zone, in 9 and 15 meters of water depth, in a line perpendicular to the coast. A sea-floor platform was deployed at each site to measure ocean currents, wave motions, acoustic and optical backscatter, temperature, salinity, and pressure. The objective was to quantify the hydrodynamic forcing for sediment transport and the response to such forcing near the seabed in the vicinity of an unmaintained inlet.

Introduction

Coastal inlets are unique features that affect the nearshore current and waves, resulting in changes to the along- and across-shelf movement of material. To better understand these systems and how they respond to storm events, the U.S. Geological Survey made time-series measurements of oceanographic, water-quality, sea-floor bedform movement, and meteorological parameters from fixed stations offshore of Matanzas Inlet, Florida, in winter 2018. The parameters measured include single-point and profiled water velocity (ocean currents), subsurface water pressure, turbidity, hydrographic parameters, and movement of sediment at the sea floor. Wave spectra and statistics were calculated from water velocity and subsurface pressure measurements. Buoy-mounted meteorological sensors also collected data as part of this study; parameters measured include wind speed, gust, and direction; air temperature; barometric pressure; relative humidity; and shortwave solar radiation.

Two sites are identified by mooring identification numbers and site identification names (table 1). The sites are oriented along a line perpendicular to the coast, offshore of the surf zone in approximately 9 and 15 meters (m) (labeled “shallow” and “deep”) of water depth (fig. 1). Each site included a heavily instrumented, quadrupedal platform (“quadpod”) and guard buoy. The platforms were approximately 2.5 m high and 2.5 m wide (figs. 2 and 3) and were designed by Jay Sisson of the Woods Hole Oceanographic Institution. Most of the pressure cases for batteries and data loggers were secured approximately 1.5 m above the seabed on horizontal channels within each platform. This design prevents the equipment from interfering with the hydrodynamics in the region of interest: the sediment resuspension layer directly above the seabed. Instruments to measure turbidity, temperature, and salinity and to image the seabed were attached to the platform legs, with careful attention to minimizing the creation of wakes in the flow field. Both buoys served to mark the underwater locations of the platforms and support measurements near (temperature and salinity) or above (meteorological measurements) the surface. The buoy at the deep site (Mooring Systems model

Table 1. Deployment and location information for platforms deployed offshore of Matanzas Inlet, Florida from January 24 to April 13, 2018.

[ID, identification number; N, north; W, west; m, meter]

Mooring ID	Site ID	Platform type	Latitude (N)	Longitude (W)	Depth (m)
1109	Shallow	Top-hat buoy	29.7114	81.2184	8.1
1110	Shallow	Large quadpod	29.7114	81.2186	8.6
1111	Deep	2-m foam buoy	29.7136	81.2138	15.3
1112	Deep	Large quadpod	29.7133	81.2146	14.9

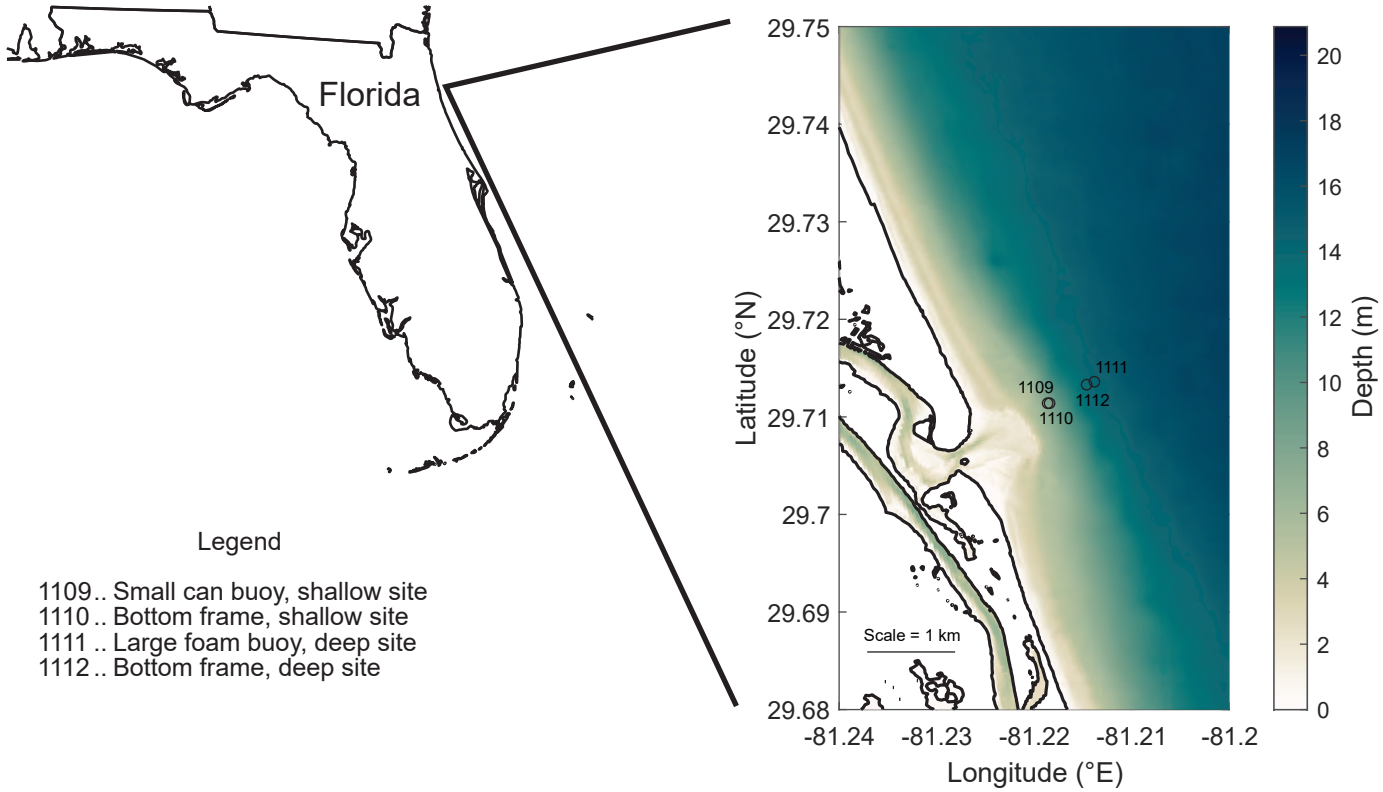

Figure 1. Study area near Matanzas Inlet, Florida. The State outline is shown at the left with the inset at right, displaying the local bathymetry and site locations "shallow" (mooring numbers 1109 and 1110) and "deep" (mooring numbers 1111 and 1112). km, kilometer; m, meter.

G2000) was 1.5 m diameter foam with a 2.1 m high tower and 0.8 m high base (fig. 4). A smaller surface top-hat buoy, similar to a small navigation buoy was used at the shallow site.

To supplement the data summarized in this report, sediment samples were collected at both sites using a Shipek grab sampler and processed for grain-size information using a Horiba LA–960A laser-diffraction particle-size analyzer with a slurry sampler. Results of the laboratory analysis of the grab samples are available in Suttles and others (2021).

Site Description

This study sought to explore inlet dynamics and expand our knowledge of how storms may affect sediment stability near an inlet. Matanzas Inlet is a natural, unmaintained inlet on the Florida Atlantic coast, south of St. Augustine. Much of the east coast of the United States is developed, so this experiment at Matanzas Inlet was a unique opportunity to study inlet dynamics at a natural setting. The dynamics of interest are the interaction of outflowing fresh water from the Matanzas River with the tides, currents, and waves encountered beyond the river mouth. Being unmaintained was an important factor in choosing this inlet for study. Inlets maintained for commercial and recreational boating are altered by anthropogenic forces, and the bathymetry of these systems may not be representative of the natural hydrodynamic processes that were measured, likely causing errors in the estimates of sediment transport. Sediment fluxes may be driven by a variety of factors, such as along-shore flow, tidal flow, and wave-induced bottom stress. The flux, as the cause of sediment accretion or erosion, influences inlet stability and migration.

The two deployment sites were slightly north of the inlet mouth (fig. 1), on a line perpendicular to both the shoreline and bathymetric contours. The "shallow" site was 840 meters from shore between the 8- and 9-meter depth contours. The "deep" site was 1,300 meters from shore at the 15-meter depth contour. The sea floor at the shallow site was primarily composed of medium-fine sand, and at the deep site it was composed of a finer grained silty sand (Suttles and others, 2021). This sediment is subject to resuspension in storms or times of increased currents or waves. The bathymetry in the area showed a consistent 1:100 gradient deepening offshore. Additional sediment deposits with complicated structure were observed at the mouth of the inlet.

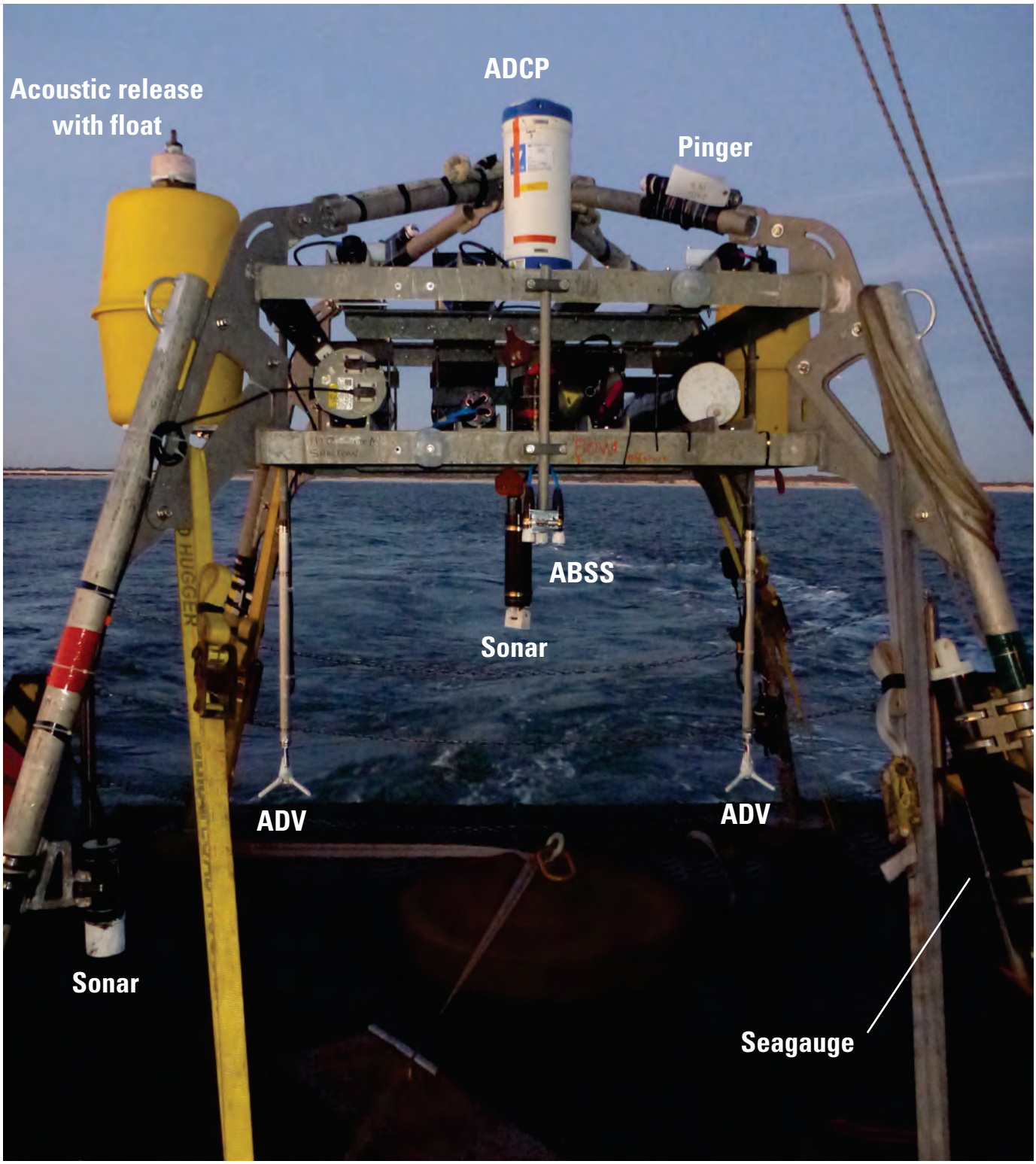

Figure 2. The instrumented sea-floor platform prior to deployment at the Matanzas Inlet, Florida, shallow site. The two Imagenex sonars, Nortek acoustic Doppler velocimeters (ADVs), Aquatec Aquascat acoustic backscatter sensor (ABSS), upward-looking acoustic Doppler current profilers (ADCPs), acoustic pingers, Sea-Bird Seagauge, and acoustic release recovery system are shown in this view. Photograph by Ellyn Montgomery, U.S. Geological Survey.

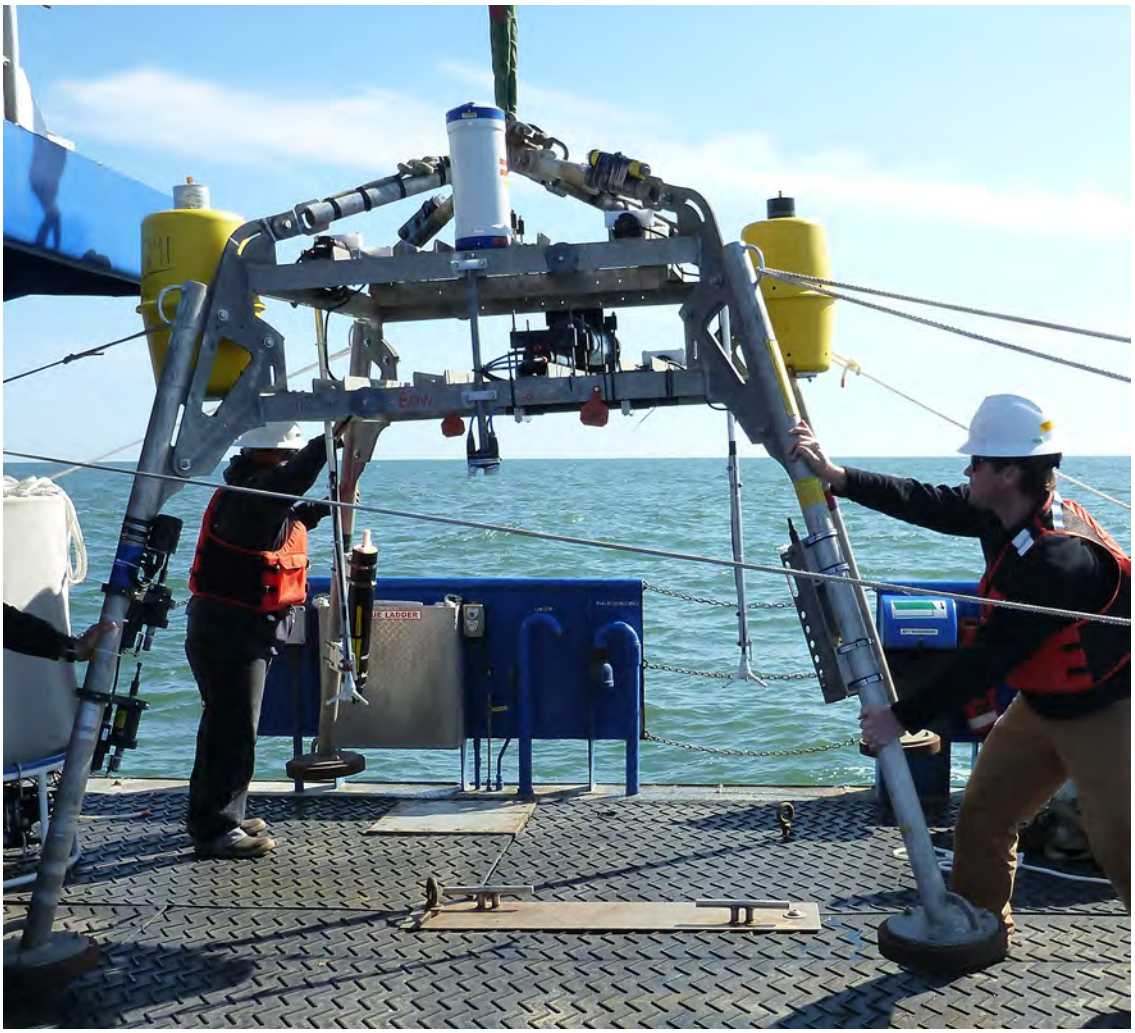

Figure 3. Instrumented sea-floor platform being moved on deck prior to deployment at the Matanzas Inlet, Florida, deep site. Photograph by Ellyn Montgomery, U.S. Geological Survey.

Instruments

Autonomous instruments, with internal power and memory, were deployed at the two sites from January 24 to April 13, 2018, to measure the current velocity structure outside the surf zone near the Matanzas Inlet and the effects on sediment transport in response to periodic storm events. The instruments on the bottom platforms (figs. 2 and 3) measured ocean currents, wave motion, acoustic and optical backscatter, temperature, salinity, and pressure to quantify the forcing for sediment transport and response near the seabed. Two sonars operating at different frequencies were mounted on the platform at the shallow site to record how the sea-floor bedforms responded to ambient conditions.

The larger buoy at the deeper site supported meteorological measurement of local atmospheric conditions during the study (fig. 4), and both buoys measured near-surface water temperature and salinity. The processed time-series data that are reported here are presented in six categories: (1) currents (profiles and, in the case of the acoustic Doppler velocimeter [ADV], single-point water velocities), (2) wave statistics, (3) backscatter, (4) imaging sonar, (5) seawater temperature and salinity, and (6) meteorological observations.

The following instruments, with measured parameters, were used to collect time-series data in this study:

- Nortek Aquadopp high-resolution (HR) acoustic Doppler current profiler (ADCP): current profiles
- Nortek Signature acoustic Doppler current profiler (ADCP): current profiles
- Nortek Vector acoustic Doppler velocimeter: single-point current measurements
- TRDI–V acoustic Doppler current profiler (ADCP): current profiles, waves (directional)
- Sea-Bird model SBE 26 Seagauge: waves (nondirectional)

Figure 4. Surface buoy with meteorological sensors deployed at the deep site off Matanzas Inlet, Florida. Photograph by Ellyn Montgomery, U.S. Geological Survey.

- Sea-Bird model SBE 37–SM MicroCAT: temperature and conductivity
- Aquatec model Aquascat acoustic backscatter sensor: acoustic backscatter profiles
- Aquatec model Aqualogger 200TY with Seapoint optical backscatter sensor: turbidity
- Imagenex model 881B tilt-adjusting imaging sonar: bedform evolution
- Imagenex model 881A high-frequency imaging sonar: bedform evolution
- Down East weather station: meteorology (winds, barometric pressure, air temperature, relative humidity, and shortwave solar radiation)
- Benthos pinger, to help locate the bottom platforms.

Tables 2–7 provide information on instruments used at each site, elevation above the seabed, and available processed results.

Currents and Waves

Both sea-floor platforms supported several instruments that measured ocean properties at different depths as well as concurrent depths, and the sea-floor platforms were spatially separated for gradient computations. An upward-looking

Table 2. Links to processed water flow (current velocity) data, by site and instrument, for platforms deployed offshore of Matanzas Inlet, Florida, from January 24 to April 13, 2018.

[Data files are in Suttles and others (2019). ID, identification number; no., number; mab, meters above bottom; ADCP, acoustic Doppler current profiler; HR, high resolution]

Mooring ID	Instrument	Serial no.	Sensor elevation (mab)	Data file
		Shallow		
1110	TRDI–V ADCP	23881	2.4	11101wh-a.nc
1110	Nortek Signature	100593	1.5	11102sig15m_iburstHR-cal.nc
1110	Nortek Signature	100593	1.5	11102sig15m_burst-cal.nc
1110	Nortek Vector	12249/5086	0.6	11109vecs-a.nc
		Deep		
1112	TRDI–V ADCP	23857	2.4	11121wh-a.nc
1112	Nortek Aquadopp HR	5374	1.5	11122HRaqd15m-a.nc
1112	Nortek Vector	11716/5096	0.6	11127vecs-a.nc
1112	Nortek Vector	12944/5243	0.6	11128vecs-a.nc

Table 3. Links to processed wave (directional and nondirectional) data, by site and instrument, for platforms deployed offshore of Matanzas Inlet, Florida, from January 24 to April 13, 2018.

[Data files are in Suttles and others (2019). ID, identification number; no., number; mab, meters above bottom; Y, yes; N, no]

Mooring ID	Instrument	Serial no.	Sensor elevation (mab)	Data file	Direction
		Shallow			
1110	TRDI–V ADCP	23881	2.4	11101whVp-cal.nc	Y
1110	Sea-Bird SBE 26 Seagauge	1378	0.4	111010sgw-cal.nc	N
		Deep			
1112	TRDI–V ADCP	23857	2.4	11121whVp-cal.nc	Y
1112	Sea-Bird SBE 26 Seagauge	1099	0.4	11129sgw-cal.nc	N

TRDI–V current velocity profiler was mounted on each platform at 2.4 meters above bottom (mab) (transducer height) to record the current profiles and wave statistics (height, period, and direction). The TRDI–V current velocity profilers were configured to measure the current profiles at 15-minute intervals and collect bursts of velocity and pressure data at hourly intervals for directional wave analysis. The burst data are provided in Suttles and others (2019) and included in appendix 1 for reader convenience. Wave statistics for both sites were calculated from the TRDI–V current velocity profiler's beam velocity profiles and pressure, sampled at 2 hertz (Hz) for 4,096 samples (34.13 minutes) every hour. Each platform also had a down-looking current velocity profiler to measure current profiles within 1 meter of the sea floor; both downward-looking current velocity profilers recorded burst data that were averaged after recovery from 120-second subsamples from the top, quarter and bottom of each hour. On the shallow platform, a Nortek Signature current velocity profiler sampled in 2 centimeter (cm) vertical beam bins and 20 cm slant beam bins, with hourly bursts of 8,192 points sampled hourly at 4 Hz; on the deep platform, a Nortek Aquadopp high-resolution current velocity profiler sampled in 5-cm vertical bins with hourly bursts of 4,096 points sampled at 2 Hz.

Each platform also had a Sea-Bird SBE 26 Seagauge Wave and Tide Recorder mounted at 0.4 mab to measure pressure with Paroscientific Digiquartz sensors, which have an accuracy of 0.01 percent of the full measurement range of the sensor. The Sea-Bird SBE 26 Seagauge at the shallow site had a 30-m full scale, and the one at the deep site had a 130-m full scale. They sampled in hourly bursts of 4,096 points at 2 Hz. Nondirectional wave statistics and tidal elevations were computed from the pressure burst data.

Table 4. Links to processed acoustic and optical backscatter, by site and instrument, for platforms deployed offshore of Matanzas Inlet, Florida, from January 24 to April 13, 2018.

[Data files are in Suttles and others (2019). ID, identification number; no., number; mab, meters above bottom, ABSS, acoustic backscatter sensor]

Mooring ID	Instrument	Serial no.	Sensor elevation (mab)	Data file
		Shallow		
1110	Aquatec Aquascat ABSS	910-131	1.3	11103abss15m-a.nc
1110	Nortek Signature	100593	1.5	11102sig15m_echo1-cal.nc
1110	Aqualogger 200TY	371-002/1875	0.74	11106slb-a.nc
1110	Aquatec Aqualogger 200TY	371-025/635	0.4	111011slb-a.nc
		Deep		
1112	Aquatec Aquascat ABSS	910-130	1.3	11123abss15m-a.nc
1112	Aquatec Aqualogger 200TY	371-004/144	0.9	11124slb-a.nc
1112	Aquatec Aqualogger 200TY	371-027/240	0.6	11126slb-a.nc

Table 5. Links to sonar data collected at the shallow site offshore of Matanzas Inlet, Florida, from January 24 to April 13, 2018.

[Data files are in Suttles and others (2019). ID, identification number; no., number; mab, meters above bottom.]

Mooring ID	Instrument	Serial no.	Sensor elevation (mab)	Data file
		Shallow		
1110	Imagenex 881B imaging sonar	1751	1.0	11104fan_raw.cdf
1110	Imagenex 881A high-frequency imaging sonar	5908	0.45	11107hffan_raw.cdf

Table 6. Links to processed seawater temperature and conductivity data, by site and instrument, for platforms deployed offshore of Matanzas Inlet, Florida, from January 24 to April 13, 2018.

[Data files are in Suttles and others (2019). ID, identification number; no., number; mab, meters above bottom]

Mooring ID	Instrument	Serial no.	Sensor elevation (mab)	Data file
		Shallow		
1109	Sea-Bird SBE 37 MicroCAT	706	7.5	11091mc-a.nc
1110	Sea-Bird SBE 37 MicroCAT	3575	0.75	11105mc-a.nc
		Deep		
1111	Sea-Bird SBE 37 MicroCAT	465	14.2	11112mc-a.nc
1112	Sea-Bird SBE 37 MicroCAT	681	0.75	11125mc-a.nc

Table 7. Link to meteorological data collected at the deep site offshore of Matanzas Inlet, Florida, from January 24 to April 13, 2018.

[Data files are in Suttles and others (2019). ID, identification number; no., number; m, meter (above sea surface)]

Mooring ID	Instrument	Serial no.	Sensor elevation (m)	Data file
		Deep		
1111	Down East weather station	USGS-2	-2.5	11111met-a-fix.nc

Finally, both platforms had two additional Nortek Vector velocimeters mounted 0.5 mab and separated by 2 m horizontal distance. The shallow bottom frame was deployed such that the velocimeter probes were aligned parallel to the shoreline. Each velocimeter collected hourly bursts of 32,768 points sampled at 16 Hz.

The Nortek Aquadopp, Nortek Signature, Nortek Vectors, and Sea-Bird Seagauge instruments all operated for the complete duration of the deployment (about 2.5 months). Unfortunately, the TRDI–V at the shallow site failed to get power from its external battery, so its record ends early on February 23 (about 1 month). The TRDI–V at the deep site functioned throughout the deployment; however, it experienced intermittent power failures throughout due to a poor power connection with the external battery. This created 1- to 2-minute gaps in some of the burst data. Wave statistics were calculated from bursts that were complete. The entire raw burst datasets are released for completeness.

Backscatter (Turbidity)

Both sea-floor platforms supported sensors to evaluate turbidity using acoustic and optical methods. To record acoustic backscatter profiles, downward-looking Aquatec Aquascat acoustic backscatter sensors with three transducers (0.5, 2.5, and 4.0 megahertz [MHz]) were mounted on each quadpod at 1.3 mab. Each acoustic backscatter sensor recorded hourly bursts of 2,048 samples at 2 Hz in 1-cm depth bins. Like the velocity data, these data were also averaged after recovery from 120-second subsamples, but only at the top and quarter hour since these bursts were only 1,024 seconds long.

On each bottom platform, optical backscatter was measured by two Aquatec Aqualoggers with Seapoint optical backscatter sensors mounted on one leg. These were placed at 0.74 and 0.4 mab at the shallow site and 0.9 and 0.6 mab at the deep site. Only the upper sensor on the shallow platform logged data for the entire deployment, but three others recorded data that passed quality assurance and control for almost the whole duration. Data from the lower sensor on the shallow platform end on April 5, when the head was sheared off. On the deep platform, both optical sensors became fouled during the deployment; data that passed quality assurance and control recording from the upper sensor end on April 2, and from the lower sensor they end on March 9.

Sonar Bedform Imaging

The sea floor at the shallow platform was expected to be more dynamic, so both Imagenex sonars were mounted there. It had two imaging sonars with different frequencies to enable robust data collection over the widest range of conditions. The high-frequency sonar, operated at 2.25 MHz, was mounted on a leg at 0.45 mab and imaged the seabed every 30 minutes. The low-frequency sonar, operated at 1.33 MHz, was mounted between two adjacent legs at 0.96 mab and imaged the seabed every hour. Both sonars operated for the full duration of the deployment. The regions imaged by the sonars overlapped so that stereoscopic techniques could be employed to analyze ripple size, shape, and orientation.

Temperature, Conductivity

Sea-Bird MicroCATs were attached to the underwater structure of the buoys at both sites to measure near-surface water temperature and conductivity every 5 minutes. A MicroCAT was also mounted on each quadpod at 0.75 mab to record data near the other near-sea-floor observations. All four MicroCATs recorded data throughout the deployment. The conductivity cell on the shallow platform clogged during a storm on February 11, after which no salinity data are available.

Meteorological Observations

At the deep site a buoy-mounted weather station made by Down East provided local meteorological conditions during the study period. The sensors were mounted 2.5 meters above the sea surface, and they measured air temperature, barometric pressure, wind speed and direction, relative humidity, and shortwave radiation throughout the deployment.

Antifouling

The optical and acoustic sensor transducers and the sonar heads were covered with zinc oxide paste just prior to deployment to discourage the settling and growth of organisms.

Data Processing

All the deployed instruments were autonomous, with internal data storage. After recovery, data were offloaded from the instruments. Manufacturers' software was used to apply calibration coefficients and convert the data to scientific units. These output files were then converted by custom, instrument-specific MATLAB programs to Equatorial Pacific Information Collection (EPIC) convention-compliant Network Common Data Form (netCDF) files for release and distribution on the U.S. Geological Survey Oceanographic Time-Series Data Collection website. Files listed in this report are available in Suttles and others (2019); links provided in the tables are for reader convenience. Additional information on data processing, quality assurance and control protocols, file formats, nomenclature, and access methods used is provided in Montgomery and others (2008).

All subsurface pressure data (data from the TRDI–V ADCPs, Nortek Signature, Nortek Vector, Nortek Aquadopp, and Sea-Bird Seagauge instruments) were corrected for changes in atmospheric pressure by using local barometric pressure data from the meteorological station at the deep site (mooring number 1111). This was done to give a more accurate representation of pressure caused by the overlying water. Corrected pressure records were saved in the netCDF files with the variable name "P_1ac."

The TRDI–V current velocity profiler wave data were processed with the manufacturer's software to output spectra (pressure, surface, velocity) and these statistics (variable names are in parentheses):

- significant wave height (wh_4061)
- mean wave height (mwh_4064)
- peak period (wp_peak)
- mean period (wp_4060)
- direction of the peak wave period (wvdir)

Quality control and quality assurance checks were performed on all the data collected. Measurements that did not pass the quality control and quality assurance process were replaced with fill values in the netCDF output file. Fill values indicate nonvalid data points and are assigned a value of 1e35 for floating point variables and −32,768 for integer variables. Obvious spikes in individual parameter time series were removed by using either a recursive filter or median filter technique, in which values that changed from one time point to the next by more than a set threshold were flagged and assigned a fill value. Velocity data from the current velocity profilers and velocimeters were checked for low correlation values, which were replaced by fill values. For upward-looking current velocity profiles, velocity bins that were too close to or above the water surface were likewise assigned fill values.

Results

Time-series data quantifying currents, waves, acoustic and optical backscatter, sonar images, and meteorological conditions were collected to estimate how sediment dynamics near a natural inlet respond to periodic storms. The overall data return for the experiment exceeded 80 percent. The most common cause of data loss was instrument or sensor failures, most notably the TRDI–V at the shallow site. The other significant cause of data loss was fouling of the conductivity and temperature sensors on the MicroCATs and backscatter sensors. There was heavy barnacle and encrusting biofouling on the aluminum quadpods and the instrument housings, but the zinc oxide paste effectively prevented the encrusting organisms from attaching to the transducers (fig. 5).

Note that the platform at the shallow site rotated from its original deployment position several times during storms. The heading, pitch, and roll data from the sensors indicate the platform rotated on February 1, 3, and 13, about 5 degrees west each time, and on March 5, the platform rotated 20 degrees west (west rotation is negative or counterclockwise). This movement is accounted for in the treatment of currents and waves data and is not accounted for in the sonar image data, since the sonar data are distributed without any transformations.

The landing page for these data (Suttles and others, 2019) contains details of all field activities associated with this project, Google Earth visualizations of deployment locations, and sampling interval information. The edited, final data can be downloaded from the catalog of data web page or accessed directly at the "Data access via THREDDS" (thematic real-time distributed data services) links on the landing page. File naming conventions for time-series observations are described in appendix 1 of Montgomery and others (2008). Results from each data category are reviewed in the following subsections.

Currents

The TRDI–V current velocity profiler on the shallow platform only collected a month of data, but the other TRDI–V at the deep site worked for the full 2.5 months, providing one full record of upward-looking current profiles (fig. 6). The data from both sites show peaks in near-sea-floor currents to the south, with speeds >50 cm/s. The surface currents followed the same pattern but had more northerly excursions. The single-point current sensors (velocimeters) also provided nearly complete records for the deployment. Each site also had downward-looking current profilers within a meter of the sea floor. The combination of upward-looking and downward-looking profiles (fig. 7) allows us to gain insights about how the water is moving in the entire water column. Table 2 lists all current velocity results with links to the locations of the processed netCDF output files.

Figure 5. Biofouling on the quadpod shown compared to minimal fouling on sensors coated with zinc oxide paste (white). Photograph by Dann Blackwood, U.S. Geological Survey.

Waves

Spectra and statistics for directional waves from the TRDI–V and nondirectional waves from Seagauge pressure loggers were calculated (fig. 8). When wave energy was low and significant wave heights were small (<0.02 m), it was difficult to determine meaningful estimates of peak wave period and wave direction. During these times of low wave energy, peak period and direction estimates were often set to the fill value in the processed netCDF files. Of primary interest are the waves during storm events, when wave energy is relatively high and significant and wave heights are larger than average. In the plot with wave direction estimates (fig. 8), mean wave direction was plotted only when significant wave heights exceeded 0.10 m to make wave propagation directions clearer. Maximum significant wave height was estimated to be about 2.2 m by using data from all the sites for the entire study period. Likewise, the maximum estimated peak period was about 15 seconds. The wave direction varied from north-northeast to slightly south of east, but almost all the waves came from directly east (offshore). Table 3 contains a complete listing, with links, of the processed wave measurements.

Backscatter (Turbidity)

Acoustic backscatter profiles of the water within 1 meter above the sea floor were made by three separate transducers with different frequencies: 0.5, 2.5, and 4.0 MHz on the Aquatec Aquascat acoustic backscatter sensors and 1 MHz on the Nortek Signature acoustic Doppler current profiler. Each frequency responds to a different range of sediment grain sizes, and the frequencies are used in tandem to understand the drivers of sediment resuspension. The data from the 2.5-MHz transducer (fig. 9) indicate several sediment resuspension events (indicated by bands of lighter color) during the deployment. The changing sea-floor elevation is shown by the bright band of reflected sound at the seabed boundary near the bottom of each frame.

Optical backscatter results showed variation in turbidity with height above sea floor and in response to storms (fig. 10). The largest turbidity measurements were made by the lower sensor on the shallow platform, with levels of approximately 300 nephelometric turbidity units frequently observed. This sensor ran until April 5 (about 2 months). The upper sensor on the shallow platform ran for the entire deployment and recorded the same temporal events at slightly lower turbidities. On the deep platform, the same events were observed, though at lower levels, with the maximum at 250 nephelometric turbidity units. The lower sensor was fouled after March 9, whereas the upper one captured several more events before it became fouled after April 2. Data during these fouled periods were set to fill values.

Sonar Bedform Imaging

Both Imagenex sonars were mounted on the shallow platform underwater and were oriented to have large regions of overlap. After processing, each sonar sample describes a circle with grayscale variations indicating ripple presence and their directions. Prior to deployment, the bottom-platform sonar images were overlaid to determine the leg positions in each image, allowing them to be aligned. The sonars were

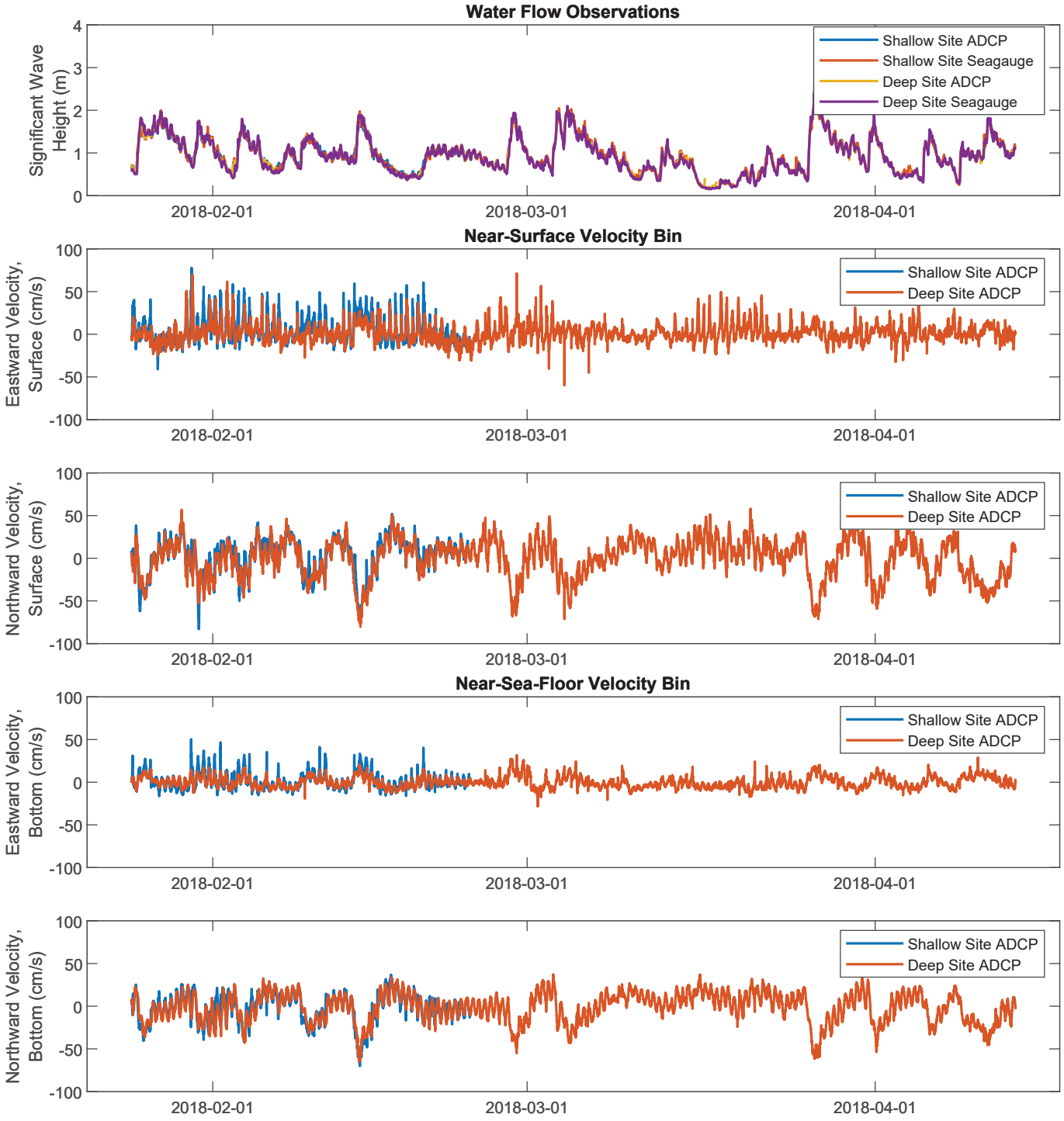

Figure 6. Current data from the acoustic Doppler current profilers (ADCPs) from both platforms, showing near-surface and near-sea-floor observations, along with significant wave height in the top frame, Matanzas Inlet, Florida (Suttles and others, 2019). cm/s, centimeter per second; m, meter.

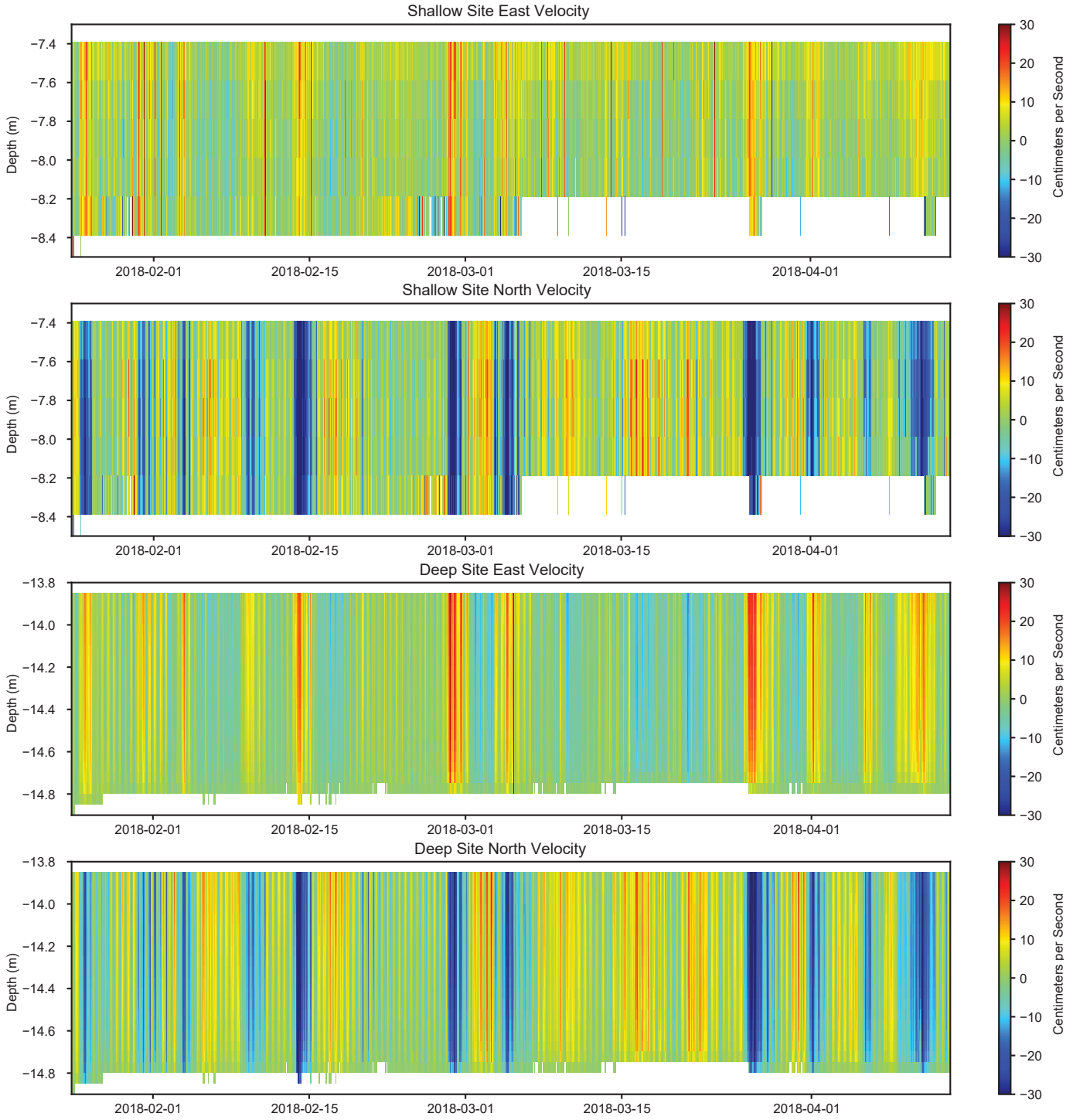

Figure 7. Profiles of east and north components of velocity from the downward-looking acoustic Doppler current profilers above the sea floor, Matanzas Inlet, Florida (Suttles and others, 2019). m, meter.

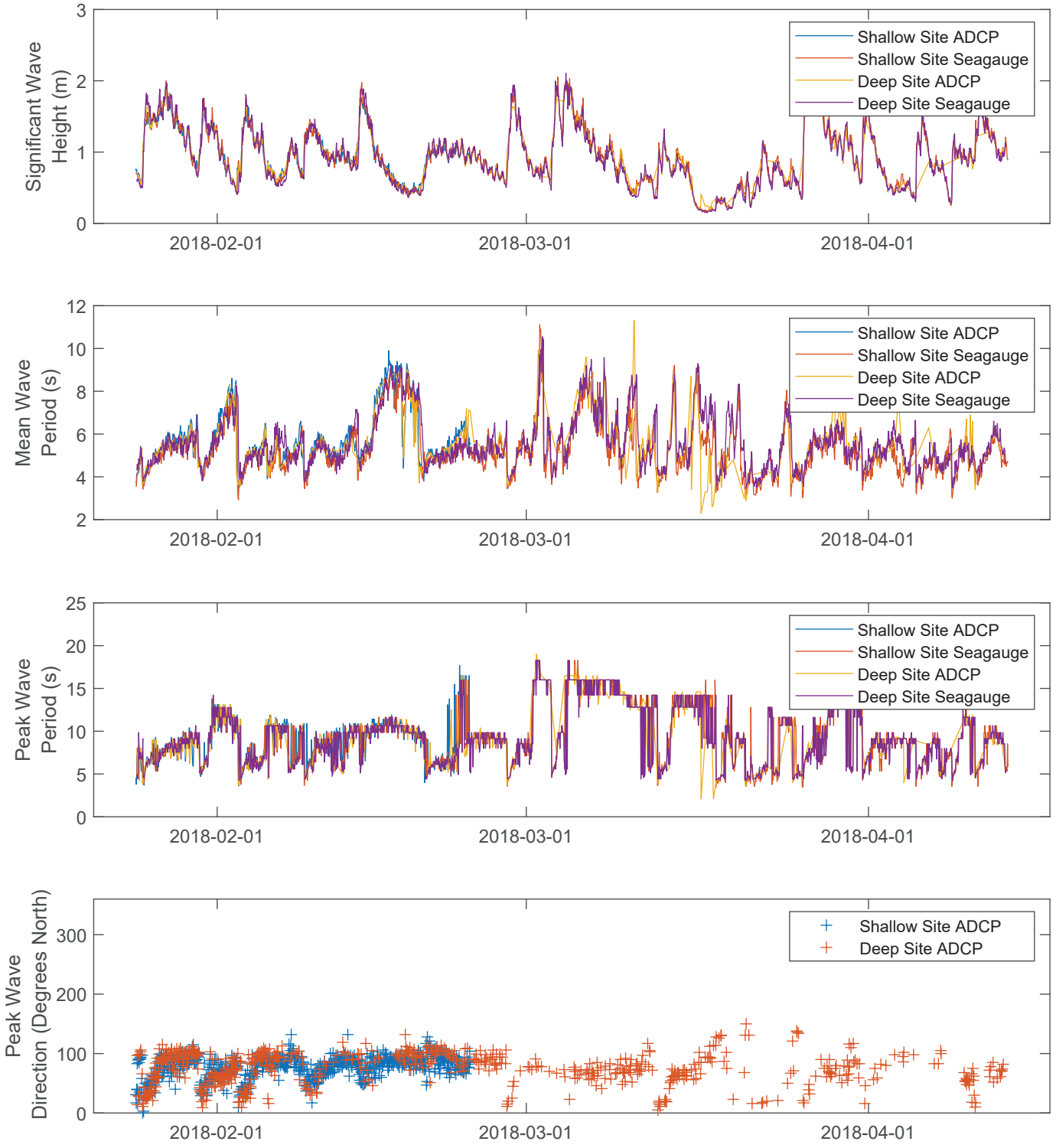

Figure 8. Wave statistics from upward-looking acoustic Doppler current profilers (ADCPs, directional) and Sea-Bird Seagauge (nondirectional) pressure loggers at both sites, Matanzas Inlet, Florida (Suttles and others, 2019). m, meter; s, second.

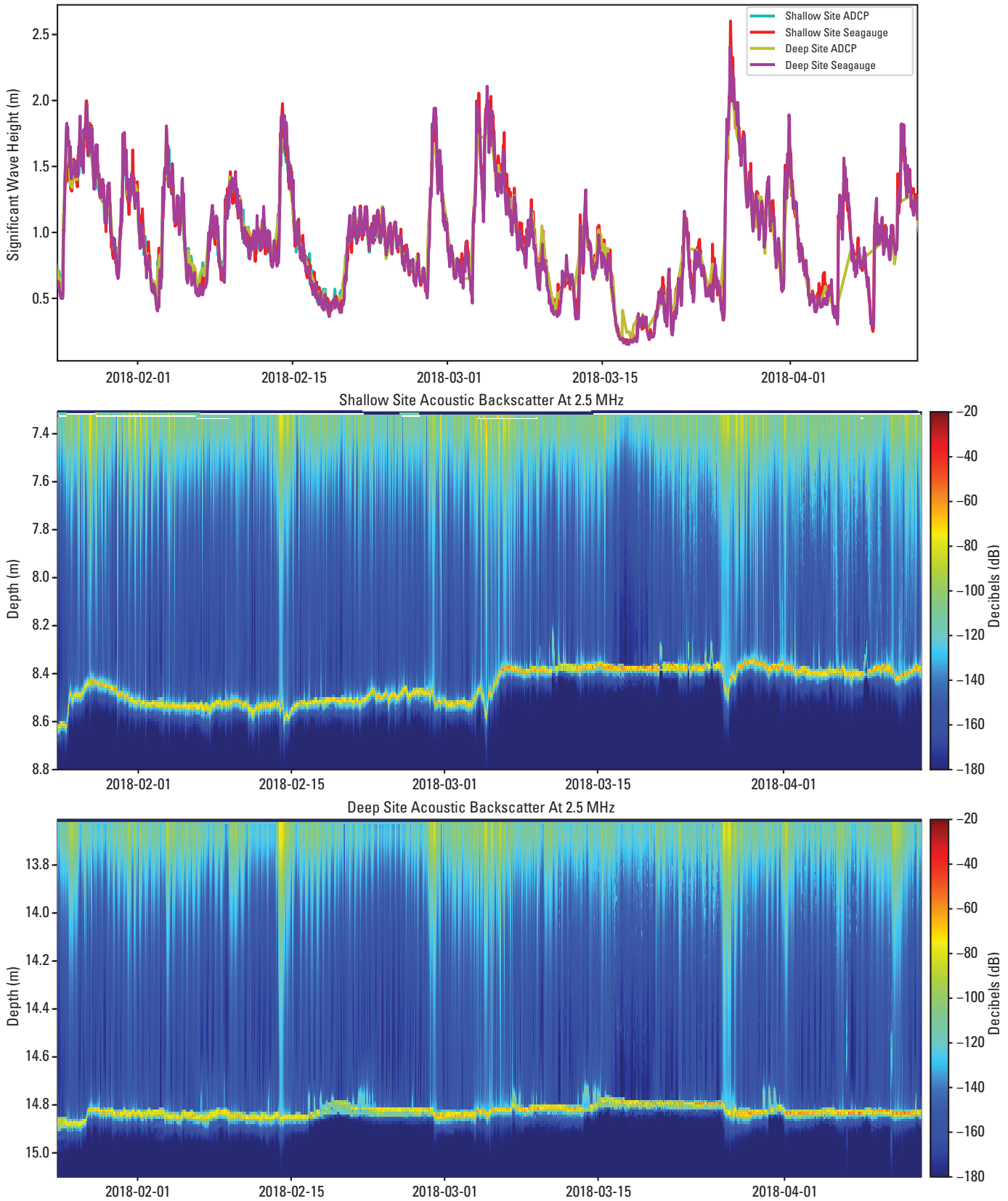

Figure 9. Profiles of acoustic backscatter at 2.5 megahertz (MHz) for both sites, Matanzas Inlet, Florida are compared with significant wave height from upward-looking acoustic Doppler current profilers (ADCPs, directional) and Sea-Bird Seagauge (nondirectional) pressure loggers at both sites, Matanzas Inlet, Florida (Suttles and others, 2019). m, meter.

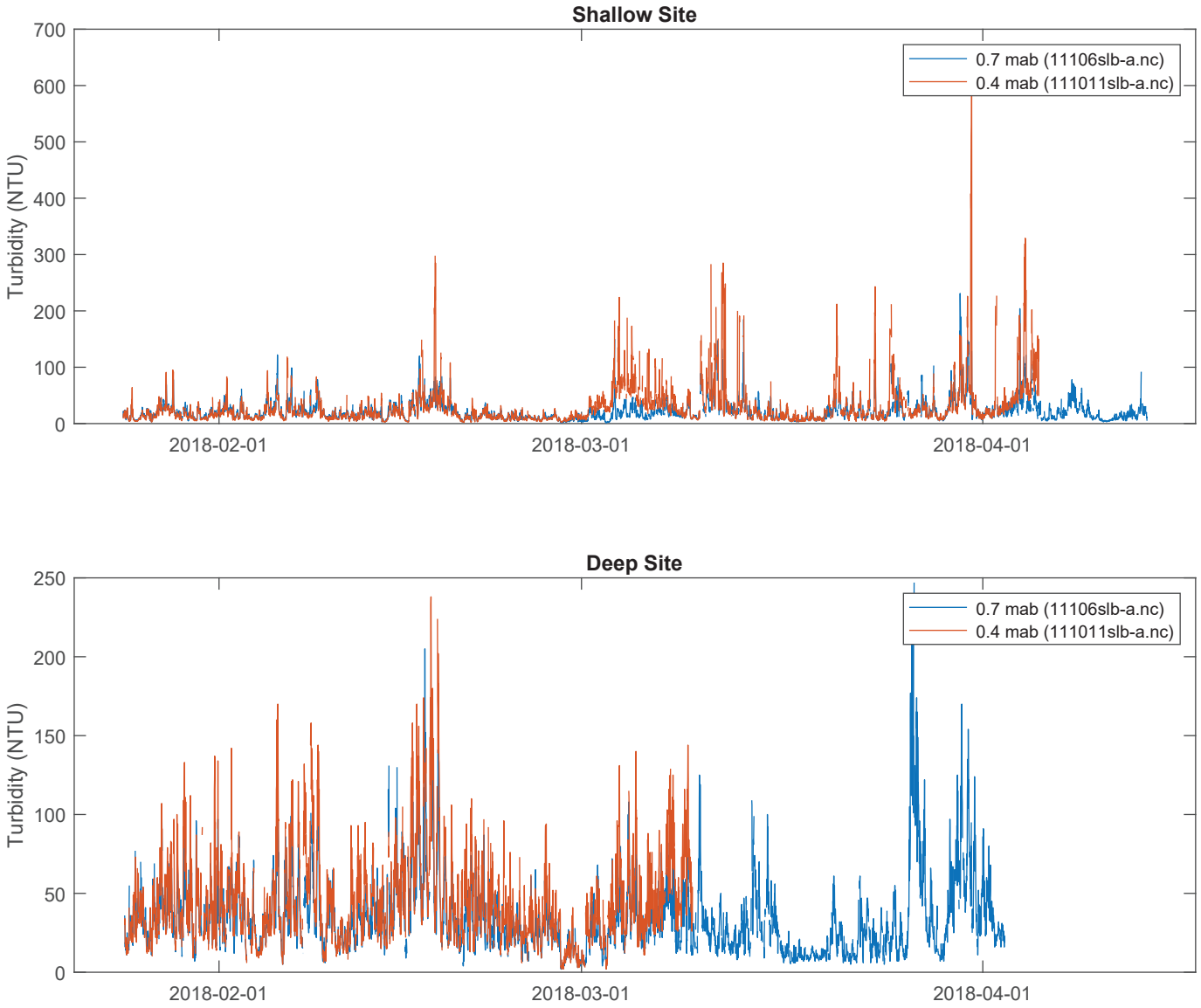

Figure 10. Near-sea-floor turbidity observations collected at both sites, Matanzas Inlet, Florida. The files from which the data were plotted are in parentheses (Suttles and others, 2019). mab, meter above bottom; NTU, nephelometric turbidity unit.

programmed to leave a thin slice of the circle empty for additional quality assurance and control. The positions of the empty zones relative to each other and the known orientations of the sonars are additional confirmation that the images are correctly rotated so that north is up (fig. 11). The image from each timestep may be assembled to make a movie, which displays migration of ripples and the occurrence of sediment resuspension events due to storms (when the suspended sediment is too dense for imaging). Note that the sonar data as released in Suttles and others (2019) are in raw form, as downloaded from the instrument. Platform movement due to storms must be accounted for when rotating the images into a Cartesian framework.

Temperature and Conductivity

Sea-Bird SBE 37–SM MicroCAT instruments, measuring conductivity and temperature, were deployed at both sites to record surface and near-sea-floor conditions. All four collected data successfully throughout the deployment (fig. 12). Near the sea floor, the conductivity cell at the shallow site became clogged on February 11, after which the sensor (11105mc) no longer recorded valid salinity data (and values were replaced with the fill value). The near-surface water temperatures showed marked daily variations, whereas the near-sea-floor sensors show less variation.

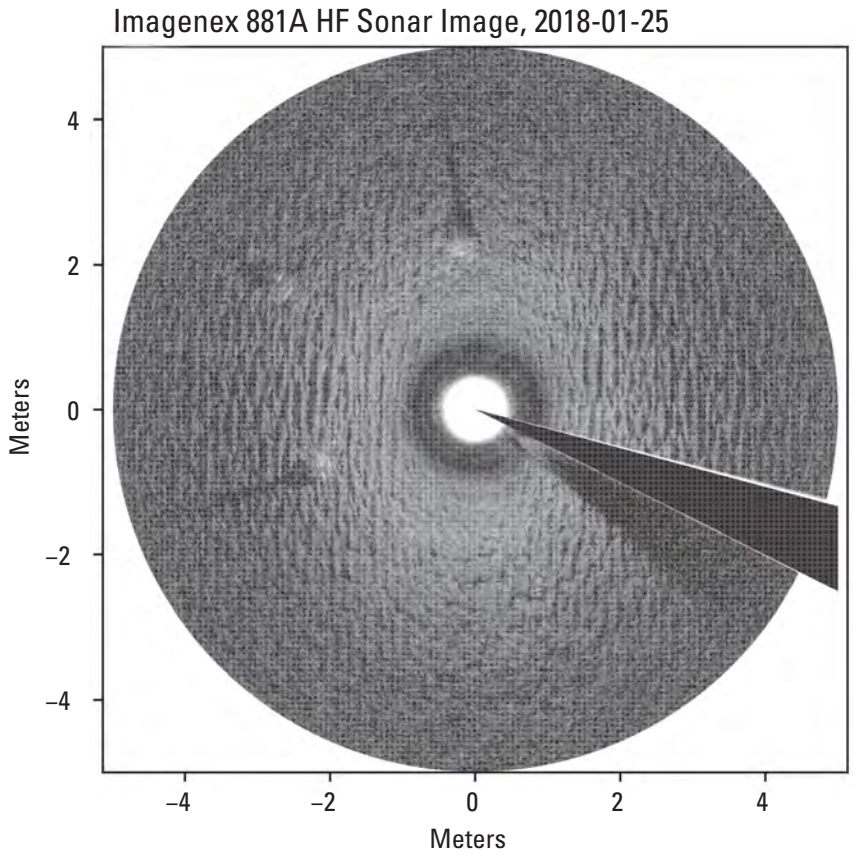

Figure 11. Example bottom image from the high-frequency (HF) sonar data showing distinct ripples on the seabed, Matanzas Inlet, Florida (Suttles and others, 2019).

Meteorological

Local meteorological conditions were recorded to provide accurate corrections to the underwater pressure measurements (figs. 13 and 14). The sensors indicate large daily variations in all measurements, overlaid by passing storms, which can be identified by wind speeds greater than 10 m/s and falling barometric pressure data. Of note are events on or near January 31, February 3, February 14, and March 4, which moved the bottom frame at the shallow site, indicated by shifts in the heading of the ADCPs.

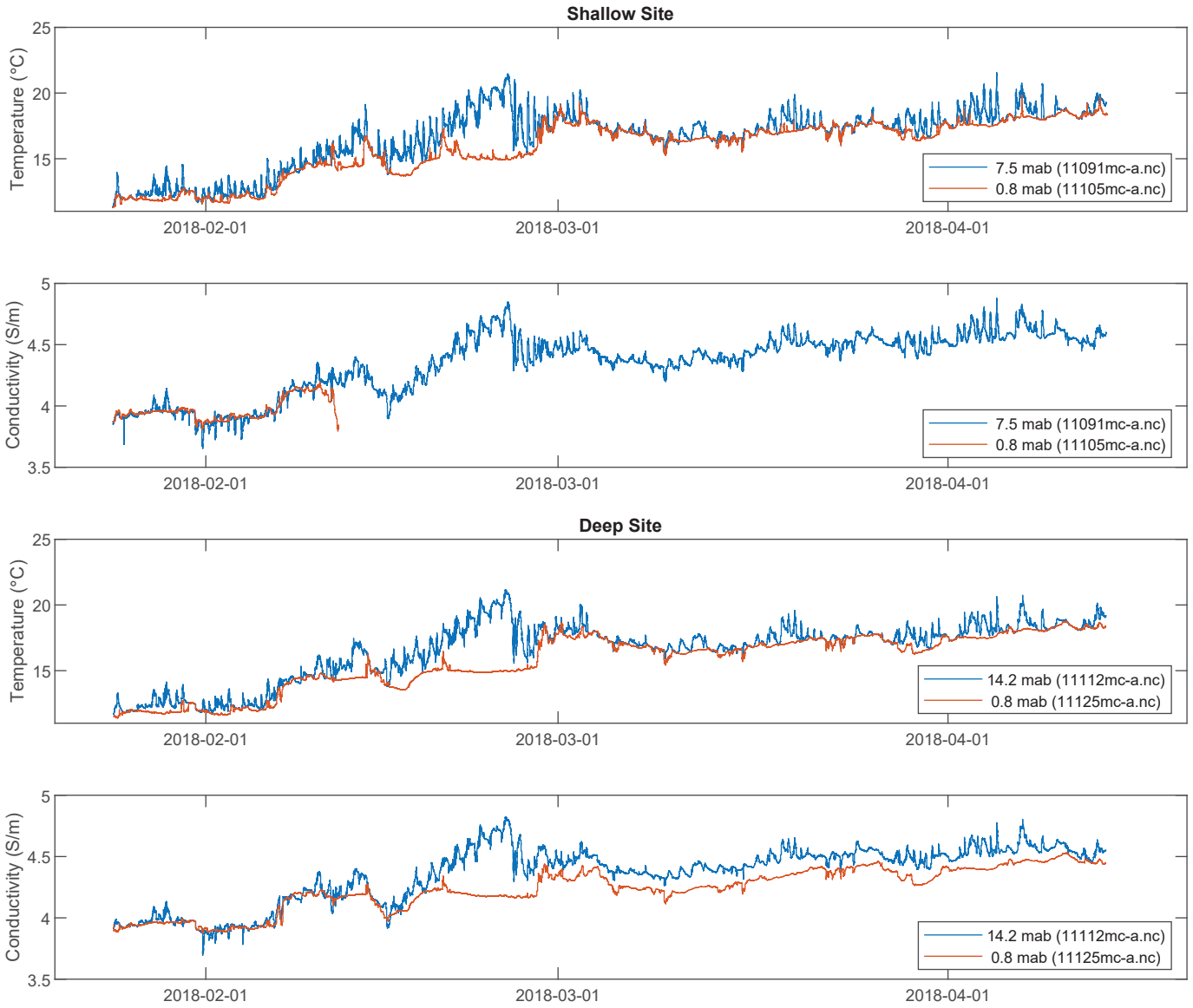

Figure 12. Temperature and conductivity measured by the MicroCATs near the surface and near the sea floor at shallow and deep sites, Matanzas Inlet, Florida (Suttles and others, 2019). The files from which the data were plotted are in parentheses. °C, degree Celsius; S/m, siemens per meter.

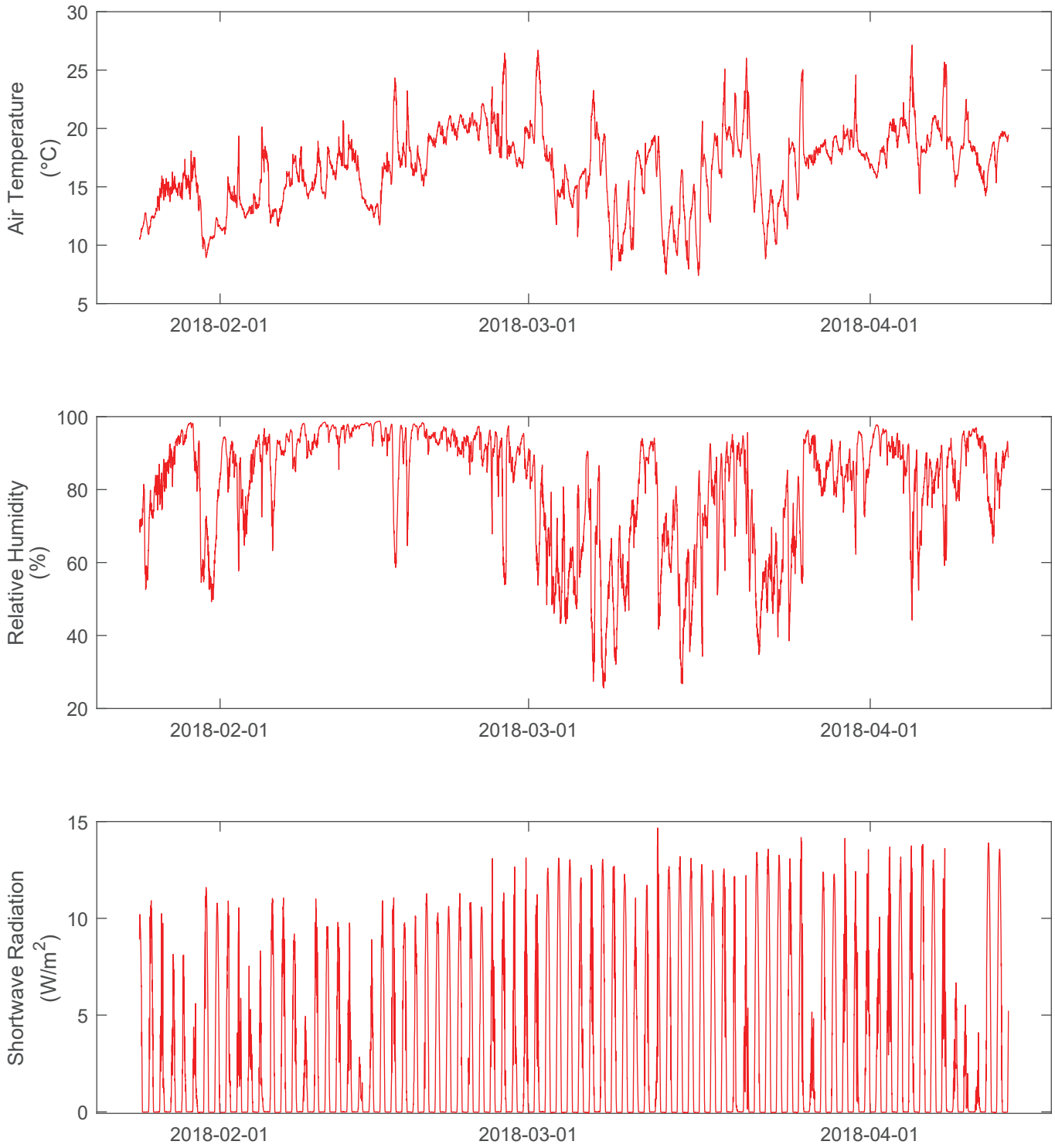

Figure 13. Air temperature, relative humidity, and shortwave radiation from the deep site, Matanzas Inlet, Florida (Suttles and others, 2019). °C, degree Celsius; %, percent; W/m^2, watt per square meter.

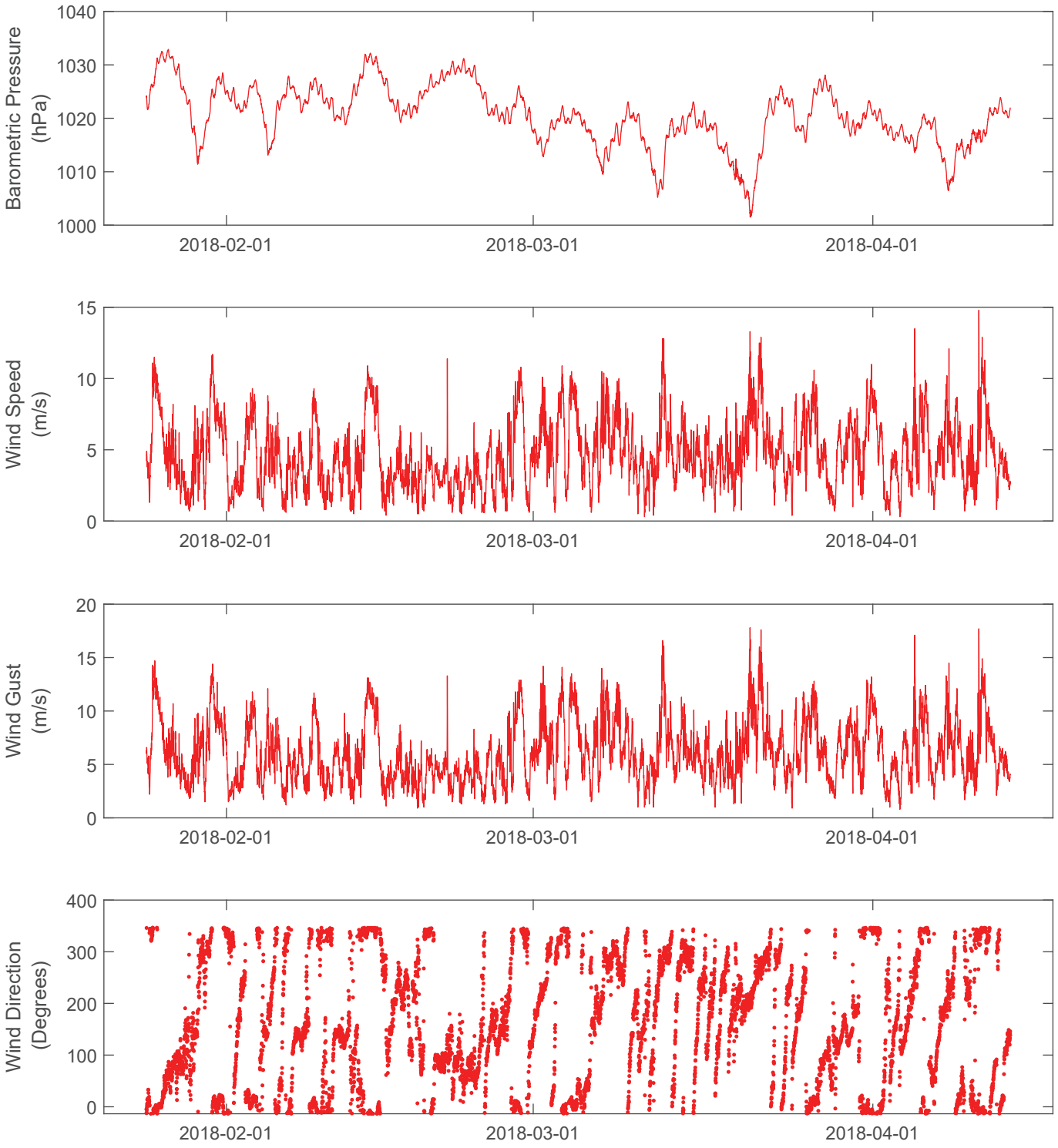

Figure 14. Barometric pressure, wind speed, wind gust, and wind direction from the deep site, Matanzas Inlet, Florida (Suttles and others, 2019). hPa, hectopascal; m/s, meter per second.

References Cited

Montgomery, E.T., Martini, M.A., Lightsom, F.L., and Butman, B., 2008, Documentation of the U.S. Geological Survey oceanographic time-series measurement database (ver. 3.0, April 2021): U.S. Geological Survey Open-File Report 2007–1194, accessed April 20, 2021, at https://doi.org/10.3133/ofr20071194.

Suttles, S.E., Warner, J.C., Montgomery, E.T. and Martini, M.A., 2019, Oceanographic and water quality measurements in the nearshore zone at Matanzas Inlet, Florida, January–April, 2018: U.S. Geological Survey data release, https://doi.org/10.5066/P9GKB537.

Suttles, S.E., De Meo, O.A., Martini, M.A, and Warner, J.C., 2021, Grain-size analysis data from sediment samples in support of oceanographic and water-quality measurements in the nearshore zone of Matanzas Inlet, Florida, 2018—U.S. Geological Survey Field Activity: U.S. Geological Survey data release, https://doi.org/10.5066/P9FKARIZ.

Appendix 1. Burst Data, Matanzas Inlet, Florida, January–April 2018

Table 1.1. Links to burst data, by site and instrument, for sea-floor platforms deployed offshore of Matanzas Inlet, Florida, from January 24 to April 13, 2018.

[Data files are in Suttles and others (2019). ID, identification number; no., number; mab, meters above bottom; ADCP, acoustic Doppler current profiler; ABSS, acoustic backscatter sensor; HR, high resolution]

Mooring ID	Instrument	Serial no.	Sensor elevation (mab)	Data file
		Shallow		
1110	TRDI–V ADCP	23881	2.4	11101whVr-cal.cdf
1110	Nortek Signature	100593	1.5	11102sigb_burst-cal.nc
1110	Nortek Signature	100593	1.5	11102sigb_echo1-cal.nc
1110	Nortek Signature	100593	1.5	11102sigb_iburstHR-cal.nc
1110	Aquatec Aquascat ABSS	910-131	1.3	11103abssb-cal.nc
1110	Nortek Vector	12249/5086	0.6	11109vecb-cal.nc
1110	Sea-Bird SBE 26 Seagauge	1378	0.4	111010sgr-cal.nc
		Deep		
1112	TRDI–V ADCP	23857	2.4	11121whVr-cal.cdf
1112	Nortek Aquadopp HR	5374	1.5	11122HRaqdb-cal.nc
1112	Aquatec Aquascat ABSS	910-130	1.3	11123abssb-cal.nc
1112	Nortek Vector	11716/5096	0.6	11127vecb-cal.nc
1112	Nortek Vector	11716	2.0	11127vectx-a.nc
1112	Nortek Vector	12944/5243	0.6	11128vecb-cal.nc
1112	Sea-Bird SBE 26 Seagauge	1099	0.4	11129sgr-a.nc

For more information about this report, contact:
Director, Woods Hole Coastal and Marine Science Center
U.S. Geological Survey
384 Woods Hole Road
Quissett Campus
Woods Hole, MA 02543–1598
WHSC_science_director@usgs.gov
(508) 548–8700 or (508) 457–2200
or visit our website at
https://www.usgs.gov/centers/whcmsc

Publishing support provided by the
Pembroke Publishing Service Center

ISSN 2331-1258 (online)
https://doi.org/10.3133/ofr20211014